OCTADECYLRHODAMINE B AS A SPECIFIC MICELLE-BINDING FLUORESCENT TAG FOR FLUORESCENCE CORRELATION SPECTROSCOPY STUDIES OF AMPHIPHILIC WATER-SOLUBLE BLOCK COPOLYMER MICELLES. SPECTROSCOPIC BEHAVIOR IN AQUEOUS MEDIA+

Jana HUMPOLÍČKOVÁ[a1], Karel PROCHÁZKA[a2,*] and Martin HOF[b]

[a] *Department of Physical and Macromolecular Chemistry and Laboratory of Specialty Polymers, Faculty of Science, Charles University, Albertov 6, 128 43 Prague 2, Czech Republic; e-mail: [1] humpolic@natur.cuni.cz, [2] prochaz@vivien.natur.cuni.cz*

[b] *J. Heyrovský Institute of Physical Chemistry, Academy of Sciences of the Czech Republic and Center for Complex Molecular Systems and Biomacromolecules, Dolejškova 3, 182 23 Prague 8, Czech Republic; e-mail: hof@jh-inst.cas.cz*

Received April 10, 2003
Accepted June 13, 2003

Fluorescence behavior of octadecylrhodamine B (ORB) and the association-dependent changes in UV-VIS absorption and fluorescence spectra in aqueous solutions were studied by UV-VIS absorption spectroscopy and steady-state and time-resolved fluorometry. Spectral changes are interpreted in terms of the hydrophobically driven formation of H- and J-dimers and higher aggregates. The knowledge gained serves as a basis for the interpretation of results of the fluorescence correlation spectroscopy study of polymeric micelles labeled with ORB.

Keywords: Octadecylrhodamine B-, H- and J-aggregates; UV-VIS absorption; Steady-state and time-resolved fluorometry; Fluorescence correlation spectroscopy; Micelles; Polymers; Dyes; Colloids.

Rhodamine-based compounds rank among to the most popular dyes, which find a broad range of applications. They have very high fluorescence quantum yields and are used, *e.g.*, as the circulation media in dye lasers[1]. Octadecylrhodamine B (ORB) is a relatively new dye which has been introduced by Molecular Probes Co., Inc., U.S.A., a couple years ago as a fluorescent dye for specific labeling of biological structures. It is fairly popular in

+ The study is a part of a long-term research of the Faculty of Science of the Charles University, MSM 1131 00001.

biochemisty and molecular biology[2], but so far it has found only a limited use for studying polymers, colloids and nanoparticles[3,4]. In this and in the accompanying paper[5], we test ORB in labeling and studying of polymeric nanoparticles by fluorescence techniques, mainly by fluorescence correlation spectroscopy.

Fluorescence correlation spectroscopy (FCS) is a relatively new spectroscopic technique that monitors behavior of fluorescent molecules, fluorescent-tagged macromolecules and nanoparticles at the molecular level in time periods ranging from 10^{-6} to 10^{-2} s. This technique was described first by Magde *et al.*[6] in 1972. In the seventies and eighties, its use was limited mostly by the lack of reliable apparatuses. Since the mid-seventies, theoretical principles of FCS and fields of its applications have been developed[7–19]. The most important advances of FCS were reviewed, *e.g.*, by Thompson[20] in 1991. With the advent of commercially available apparatuses produced by Carl Zeiss, Jena, the use of FCS spread all over the world in last ten years.

In a FCS experiment, one monitors fluorescence intensity fluctuations from a very small, irradiated volume of 10^{-18} m^3 containing a dilute solution of fluorescent particles. The fluctuations can be caused by different processes, most often by the Brownian motion, but chemical reactions, such as photobleaching, may also be a source of fluorescence fluctuations. Since the intensity of the focused laser beam is very high, the photobleaching due to the transition to the excited triplet state is a process of importance because it hinders measurement and complicates the analysis. Therefore probes with a low probability of the intersystem crossing have to be used in FCS, *e.g.*, rhodamine-based dyes. In a small irradiated volume, there are typically less than ten fluorescent particles and each time the fluorophore enters or leaves the volume, a fluctuation is registered. By monitoring the fluctuations and fitting their autocorrelation function, it is possible to evaluate the diffusion coefficient of fluorescent particles. The advantages of this technique are: (i) negligible consumption of the sample, (ii) possibility of measuring diffusion coefficients of small molecules that do not scatter light and (iii) possibility of determining diffusion coefficients of tagged molecules in mixtures and in complex systems with excess of nonfluorescent molecules. The method, however, is limited either to fluorescent or fluorescent-tagged particles with extremely low intersystem crossing rates (even fluorescein, which is described in new textbooks as a suitable probe[20] undergoes almost total photobleaching at high light intensities used in modern apparatuses).

The aim of the paper is the following. We would like to demonstrate that octadecylrhodamine B is an excellent fluorescent probe for labeling

amphiphilic core/shell structures for FCS purposes. However, its spectral behavior is very complex and, as mentioned above, it has never been studied in a broader range of conditions necessary for an unambiguous FCS research in spite of the fact that ORB is a fairly popular probe in biochemistry and biology. Therefore, we present a detailed report on its solution behavior to share the acquired knowledge with researchers that might intend to use ORB for fluorescent labeling and FCS studies on biological structures or nanoparticles in aqueous media.

EXPERIMENTAL

Materials

Octadecylrhodamine B was purchased from Molecular Probes, Inc, U.S.A.

Solvents. 1,4-Dioxane and methanol were purchased from Aldrich International and used without other purification. Deionized water was used in the study.

Techniques

UV-VIS absorption. Spectra were measured in 1-cm quartz cuvettes using a diode array UV-VIS spectrometer Hewlett–Packard, HPUV 8452A

Steady-state fluorescence spectra (*i.e.*, corrected excitation and emission spectra and steady-state anisotropy) were recorded with a SPEX Fluorolog 3 fluorometer, U.S.A., in a 1-cm quartz cuvette closed with a Teflon stopper. Oxygen was removed by 5-min bubbling with nitrogen before the measurement.

Time-resolved fluorometry. The time-correlated single photon counting technique was used for measurements of fluorescence lifetimes. The time-resolved fluorescence decays were recorded on 5000U time-resolved fluorometer (IBH, Great Britain), equipped with an IBH NanoLED-01 (490 nm peak wavelength, 1–1.5 ns in full width in the half maximum of the pulse, 1 MHz repetition rate) and cooled MCP-PMT (Hamamatsu, Japan). A deconvolution procedure was used to get the true fluorescence decays that were further fitted to multiexponential functions using the Marquardt–Levenberg non-linear least squares method using the ED software. Low values of the χ^2 (close to 1.0), and random distribution of residuals were used as criteria of the fit.

RESULTS AND DISCUSSION

Behavior of Octadecylrhodamine B in Polar Solvents

Spectroscopic behavior of common rhodamine dyes, such as rhodamine B (RB), rhodamine 6G (R6G) and rhodamine 110 (R100) in solutions and their behavior at surfaces has been the subject of numerous studies and at present their spectra are fairly well-understood[21–35]. The aforementioned dyes are soluble in polar organic solvents and little soluble in water, but

they have a strong tendency to form dimers and multiple aggregates at higher concentrations (*ca* 10^{-3} mol l^{-1} for RB [35]). Rhodamine B forms predominantly H-dimers in water and J-dimers in lower aliphatic alcohols. According to the exciton theory, the excited state of a dimer splits into two energy levels, but only one spectroscopic transition is allowed according to the structure of the dimer[30–32]. H-dimers are usually coplanar (*i.e.*, sandwich-type) nonfluorescent dimers with a blue-shifted absorption band (with respect to the monomer absorption). The non-zero electric transition moment (corresponding to the allowed electronic transition) is perpendicular to the line connecting the centers of gravity of the two aromatic ring systems. J-Dimers are fluorescent dimers with red-shifted emission. Depending on the dye and on conditions, they are either eclipsed coplanar (*i.e.*, oblique) dimers or V-shape dimers (in the limit case, they have either head-to-head or head-to-tail arrangement). The transition dipole moment of the J-dimer is parallel to the line that connects the centers of gravity of the rings. In the case of rhodamine dyes, the aromatic xanthene ring systems are not symmetrical. As a consequence, different dimers may be formed and the optical selection rules are relaxed. Both transitions (to the higher as well as to the lower excited state) are observed in the absorption spectrum, but the blue-shifted band is more intense in H-dimers, while the red-shifted one prevails in J-dimers. Possible structures of both types of dimers are depicted in Scheme 1.

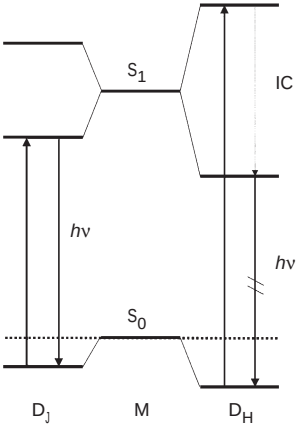

SCHEME 1
Energy levels of the ground and excited states of the fluorescent rhodamine B J-dimer (left), RB monomer (middle) and non-fluorescent RB H-dimer (right)

Since octadecylrhodamine B (Chart 1) is derived from rhodamine B, we compare our experimental results with the literature data for RB, mainly with results of Fujii *et al.* who studied RB in ethanol–water mixtures and were able to decompose experimental spectra into subspectra of monomer RB, H-dimer RB and J-dimer RB [35]. They reported a monomer absorption maximum at λ_M = 555 nm (below 10^{-4} M concentration) and the blue- and red-shifted absorption maxima of H-dimer ($(\lambda_B)_H$ = 525 nm, $(\lambda_R)_H$ = 553 nm) and $(\lambda_B)_J$ = 531 nm, $(\lambda_R)_J$ = 569 nm for J-dimer. We performed similar measurements with RB in methanol–water mixtures and we found essentially the same values.

As systematic data on the associative and spectroscopic behavior of ORB in mixed aqueous media have not been published so far, we performed a study of ORB in water–methanol solutions before attempting to investigate its binding to polymeric micelles in aqueous media. The dye is well soluble and highly fluorescent in methanol. Its monomer absorption spectrum is identical with that of RB (see Fig. 1a) and obeys the Lambert–Beer law at concentrations below 3×10^{-4} M (insert in Fig. 1a). The excitation and emission spectra are shown in Fig. 1b and the fluorescence decay in the insert in Fig. 1b. The experimental absorption coefficient, ε_{max} = 92 200 ± 700 mol^{-1} dm^3 cm^{-1} and the fluorescence decay time, τ_F = 1.7 ns.

The behavior of ORB in water and water-rich media differs significantly from that of RB. This dye behaves as a typical surfactant. We study the behavior of ORB well below the critical micelle concentration and the formation of micelles does not have to be taken into account. However, it is a

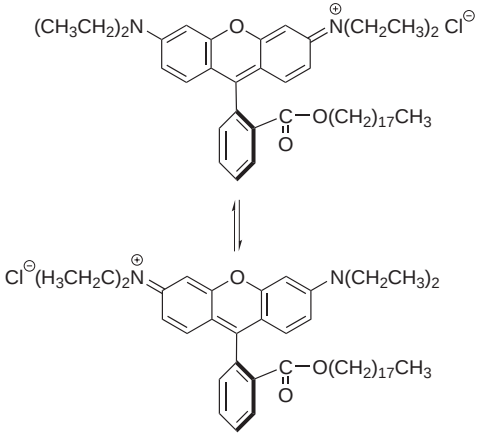

CHART 1
Structure of octadecylrhodamine B

well-known fact that surfactants with more than 12 CH_2 units form dimers (and higher associates) at concentrations considerably lower than c.m.c.[36] In ORB aggregates, individual xanthene rings come relatively close to each other and the formation of H- and J-dimers occurs therefore at very low concentrations as compared with RB. Since the aliphatic tails are reasonably flexible and assume various instantaneous conformations, we deduce that

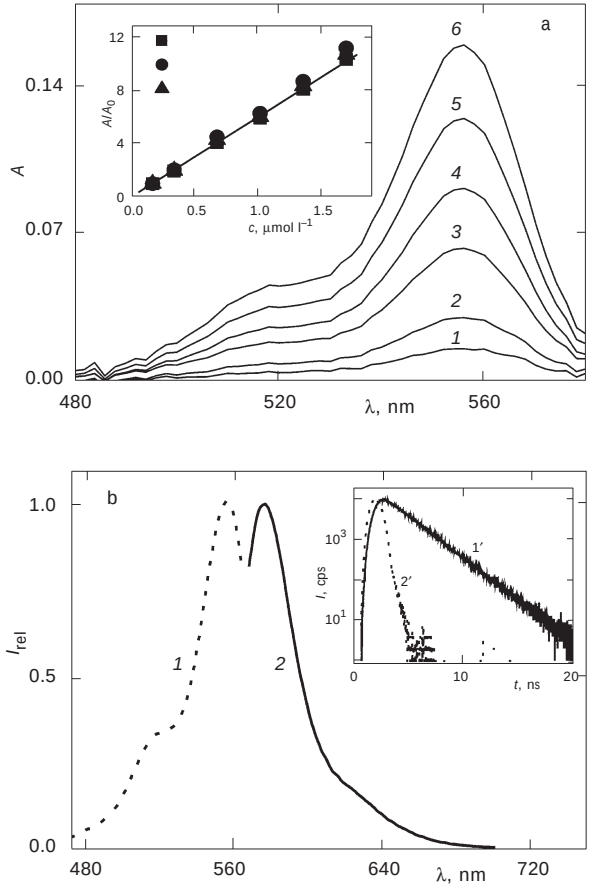

FIG. 1

a UV-VIS absorption spectra of octadecylrhodamine B solutions in methanol. c_F (mol l^{-1}): *1* 1.69×10^{-7}, *2* 3.38×10^{-7}, *3* 6.76×10^{-7}, *4* 1.01×10^{-6}, *5* 1.33×10^{-6}, *6* 1.69×10^{-6}. Insert: The Lambert–Beer plot (the ratio of absorbances A/A_0 *vs* ORB concentration, where A_0 are for $c_F = 1.69 \times 10^{-7}$ mol l^{-1}) for 522 (■), 566 (●) and 572 (▲) nm. b Normalized excitation (dotted curve *1*) and emission spectra (solid curve *2*) of ORB in methanol. Insert: Fluorescence decay at 585 nm (solid curve *1′*); excitation profile at 550 nm (dotted curve *2′*)

the microenvironments around individual fluorescent groups differ. The closely located rhodamine pairs exposed to water molecules form H-dimers, while those, which are more surrounded by aliphatic tails, tend to form J-dimers, as does RB in ethanol because the polarity of their microenvironment is lower. The above described scheme assumes that the hydro-

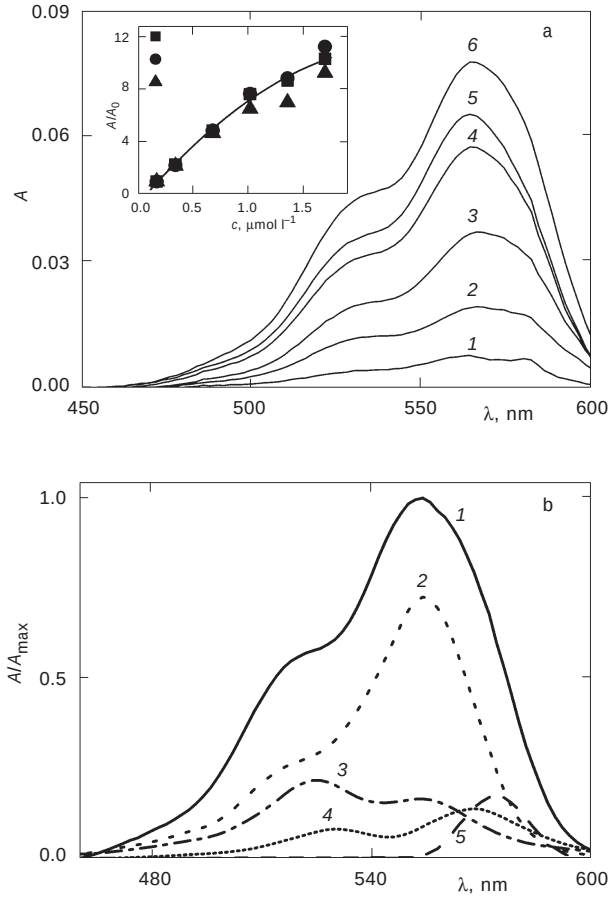

FIG. 2

a UV-VIS absorption spectra of ORB in aqueous solutions for the same concentrations as in Fig. 1. Insert: A plot A/A_0 *vs* ORB concentration in water, showing deviations from the Lambert–Beer law at 532 (●), 564 (■) and 580 (▲) nm. b The decomposition of experimental absorption spectrum of 1.69×10^{-6} mol l^{-1} ORB solution in water (curve *1*) in subspectra of individual components. The absorption spectrum of ORB in water consists of 58% of monomer (curve *2*), 17% of H-aggregates (curve *3*), 11% of J-aggregates (curve *4*) and 14% of higher aggregates spectra (curve *5*)

phobic aggregation of ORB hydrocarbon tails is the primary process and the formation of H- and J-dimers or higher aggregates of fluorescent xanthene rings is the secondary process, which takes place in the pre-organized aggregates. It will be demonstrated in the next part that the real behavior obeys the outlined scheme, but is far more complex.

The absorption spectra of ORB solutions in water were measured for concentrations from 10^{-7} to 10^{-4} M, but only the spectra for concentrations from 10^{-7} to 10^{-6} M are shown in Fig. 2a, to provide a clear picture. The main absorption band around 560 nm is slightly red-shifted as compared with ORB spectra in methanol and also with RB spectra in ethanol–water (50 vol.%) mixture published by Fujii *et al.*[35] The shift is partly due to the bulk polarity change, but also to the J-dimer formation. The spectra are significantly broadened in the red region. The red band is appreciably non-symmetric with a shoulder at higher concentrations and its shape may be characterized as a double peak with a shallow minimum around 570 nm at low concentrations. Very pronounced deviations occur also in the blue region 520–540 nm. The ratio of absorbances, A_{530}/A_{560}, is appreciably higher as compared with RB as a result of the presence of H-dimers. The changes in populations of individual species with increasing concentration and deviations from the linear Lambert–Beer plot for three selected wavelengths are apparent even at the lowest concentrations used (see insert in Fig. 2a).

The measured spectra may be reconstructed fairly well using the published spectra of the monomer and both types of dimers, except the red part close to 600 nm since none of the published spectra show significant absorption in this region. The spectral decomposition is shown in Fig. 2b. The shape of the red part of the experimental spectrum suggests that the broad non-symmetrical absorption between 540 and 600 nm is composed of two bands with maxima at 564 and 580 nm. In analogy with other authors, we assume that the latter band corresponds to higher J-aggregates[27]. The spectral reconstruction leads to the finding that both types of aggregates exist in aqueous and water-rich solutions. What is slightly surprising is the content of the individual components. The fraction of H-dimer, which is the main form of RB under the given conditions, is relatively low in all studied mixtures. The predominant forms are J-dimers and higher J-aggregates, but the fraction of ORB monomers seems to be also fairly high.

The normalized steady-state excitation (emission at the maximum of the fluorescence band, *i.e.*, at 585 nm) and emission spectra of ORB (excited at 556 nm) in pure water are shown in Figs 3a, 3b for solutions in the concentration region 10^{-7}–10^{-5} M. The ratio of excitation intensities I_{522}/I_{556} is shown in the insert (Fig. 3a), as a function of ORB concentration. The shift

in the position of the emission maximum with concentration is depicted in the insert in Fig. 3b. Excitation spectra show an increasing content of H-aggregates with increasing concentration. As concerns the analysis of the excitation bands, some precaution is needed. At 556 nm we collect mainly

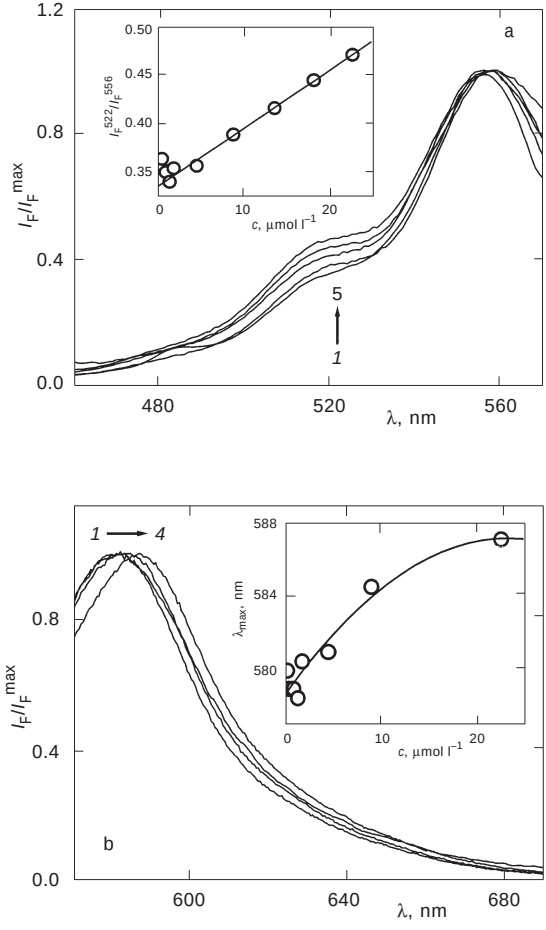

FIG. 3

a Normalized excitation ORB spectra (chosen ones) in aqueous solutions. c_F (mol l^{-1}): *1* 4.48×10^{-7}, *2* 8.64×10^{-6}, *3* 1.34×10^{-5}, *4* 1.79×10^{-5}, *5* 2.24×10^{-5}. The emission wavelength was 580 nm. Insert: The ratio of fluorescence intensities excited at 522 and 556 nm, I^{522}/I^{556} *vs* ORB concentration showing the most important changes in the shape of fluorescence spectra. b Normalized emission ORB spectra in aqueous solutions. c_F (mol l^{-1}): *1* 2.24×10^{-7}, *2* 4.48×10^{-6}, *3* 8.96×10^{-6}, *4* 2.24×10^{-5}. Excitation wavelength was 556 nm. Insert: The shift in the maximum emission wavelength λ_{max} with ORB concentration

the monomer emission. The H-dimers are non-fluorescent, but since their absorption is blue-shifted as compared with the monomer, some excited dimers (in the higher state) may transfer the excitation energy by NRET dipole–dipole interaction mechanism instead of the vibrational relaxation to the lower excitation state. Therefore we observe a NRET-sensitized increase in the excitation band of H-dimers. When monitoring the monomer emission, we observe almost no NRET contribution from the red shifted J-dimers, but there is a direct contribution resulting from the overlap of bands. Other complication consists in the fact that H-dimers (in the lower state) are efficient excitation energy traps and quench the monomer emission[37]. However, the quenching is evenly efficient for both the sensitized and direct excitation. It means that it does not weaken only the emission at maximum, but in the whole band region.

A representative fluorescence decay of ORB in water (excited at 556 nm and monitored at the maximum of the emission band, $c = 3.6 \times 10^{-6}$ mol l^{-1}) is shown in Fig. 4 (together with the excitation profile). In the concentration range 10^{-7}–10^{-5} M, the experimental fluorescence decays can be reasonably fitted by a double-exponential function, $I_F(t) = B_1 \exp(-t/\tau_1) + B_2 \exp(-t/\tau_2)$. The changes of short and long lifetimes, τ_1 and τ_2, with concentration are shown in the insert (curves *1′* and *2′*, respectively), together with the ratio

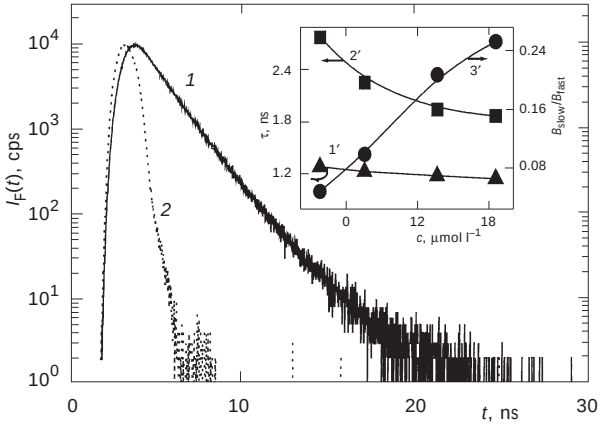

FIG. 4

A representative ORB fluorescence decay in aqueous media (solid curve *1*, $c = 3.6 \times 10^{-6}$ mol l^{-1}, excited at 556 nm and measured at 585 nm), excitation profile (dotted curve *2*). Insert: The short and long fluorescence lifetimes, τ_1 and τ_2, (curves *1′* and *2′*, respectively) and the ratio of pre-exponential factors, B_{slow}/B_{fast} (curve *3′*) obtained by double-exponential fits as functions of ORB concentration

B_{slow}/B_{fast} (curve *3′*, for the discussion of the curve – see further). Rhodamine dyes (*e.g.*, RB) are known for their high fluorescence quantum yields, both in polar organic solvents and water[20]. The fluorescence emission spectrum of ORB and its polarity shift correspond roughly to those of RB. The most remarkable difference between RB and ORB in methanol–water mixtures is the tremendous decrease in the fluorescence intensity of ORB with increasing water content (Fig. 5) due to the formation of H-dimers. As mentioned above, these dimers are not only non-fluorescent, but they are very efficient excitation energy traps and quench both the monomer and J-dimer emissions[37]. Their presence manifests itself by non-exponential emission decays (see Fig. 4) and by changes in mean fluorescence lifetimes, $\langle\tau_F\rangle$, with dye concentrations. The overall changes in fluorescence decays are complex and their unambiguous interpretation is not easy. We assume that the fluorescence lifetime of ORB is shorter in water than in methanol due to polarity change and that it is quenched by energy transfer to H-dimers. On the other hand, the monomer and J-dimer emission bands evidently overlap. Hence we observe a contribution of the J-dimer and J-aggregates decay when measuring the decay of the monomer. Since the short lifetime is almost constant, while the contribution of the longer lifetime increases with ORB concentration, we believe that the longer time corresponds roughly to J-aggregates. This is shown in the insert of Fig. 4 by the increase of the B_{slow}/B_{fast} ratio. It varies with ORB concentration since it is quenched by NRET to H-dimers. In any case, it is necessary to keep in mind

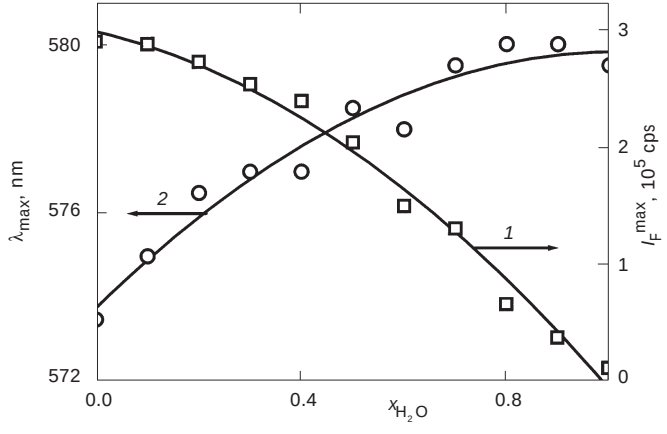

FIG. 5
Changes in fluorescence intensity (curve *1*) and the maximum fluorescence wavelength (curve *2*) with composition of the methanol–water solvent

that the double exponential function is not sufficient to describe quenched decays from a mixture of two species well. In such cases, the fitting parameters represent only some effective values and their rigorous physical interpretation is impossible.

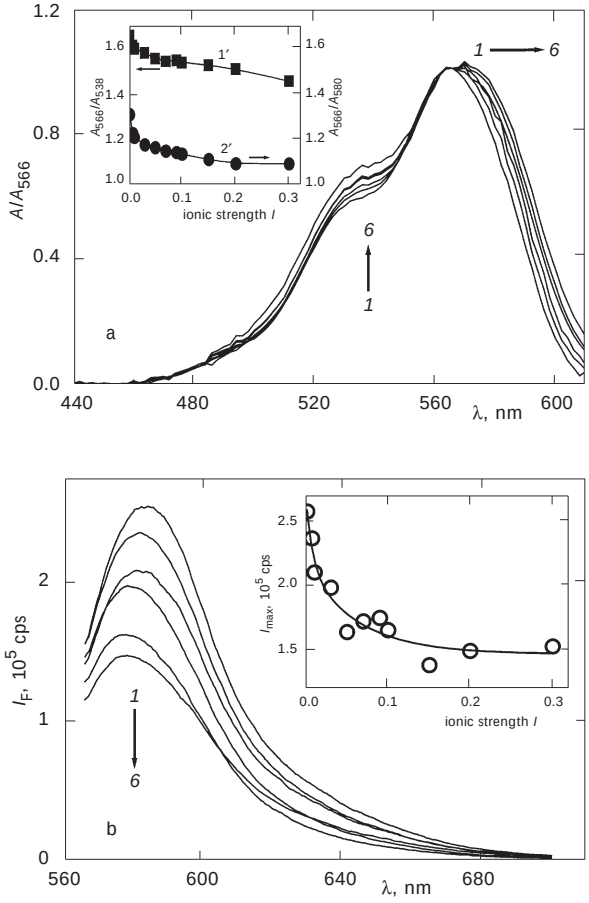

FIG. 6

a Changes in ORB absorption spectra (chosen ones) with ionic strength in NaCl solutions (c_F = 4.0 × 10^{-6} mol l^{-1}, pH 3). Ionic strength *I*: *1* 0.001, *2* 0.07, *3* 0.03, *4* 0.1, *5* 0.15, *6* 0.3. Insert: Ratio of absorbances A_{566}/A_{538} (curve *1′*) and A_{566}/A_{580} (curve *2′*) *vs* ionic strength, *I*, showing the most important changes in the shape of absorption spectra. b Changes in ORB emission spectra (chosen ones) with ionic strength in NaCl solutions (c_F = 4.0 × 10^{-6} mol l^{-1}, pH 3). Ionic strength *I*: *1* 0.001, *2* 0.007, *3* 0.01, *4* 0.05, *5* 0.05, *6* 0.2. Excitation wavelength was 556 nm. Insert: The plot of the fluorescence intensity at the maximum of the emission band, I_{max} *vs* ionic strength *I*

The maximum fluorescence intensity (curve *1*) together with corresponding wavelength (curve *2*) are depicted in Fig. 5 as functions of the solvent composition. The shape of curve *1*, *i.e.* decrease in fluorescence intensity with water content corresponds to the above discussed association and spectroscopic behavior amphiphilic dyes with long aliphatic tails, such as 5-*N*-octadecanoyl-aminofluorescein, *etc.*[38] The red shift of the maximum position with increasing water content corresponds to the polarity shift of similar dyes, although it was not reported by Fujii for rhodamine B in similar mixtures[35].

The ionic strength of the solution influences strongly the absorption and fluorescence spectra of aqueous solutions of ORB. Small ions screen electrostatic repulsion between two positively charged rhodamine ring systems. An increase in their concentration promotes the formation of aggregates which is manifested by changes in the shape of both absorption (Fig. 6a) and emission spectra (Fig. 6b) and by a decreased emission intensity due to self-quenching (insert in Fig. 6b). While the electrostatic screening effect of small ions results generally in (i) significant broadening of absorption spectra in both the blue and red regions, (ii) blue shift of the fluorescence maximum and (iii) decrease in the fluorescence intensity, some anions, *e.g.*, ClO_4^-, induce very specific time-dependent spectral changes. Since the aim of this work is to study polymer systems, the results concerning the role of inorganic ions will be published separately.

CONCLUSIONS

1. The UV-VIS spectroscopic behavior of octadecylrhodamine B in very dilute solutions in aqueous media, which was studied by absorption and fluorescence techniques, is very complex and shows that the shape and position of spectral bands is influenced by the hydrophobically driven association of amphiphilic ORB molecules.

2. Octadecylrhodamine B is a fluorescent surfactant with 18-carbon aliphatic chain. We have found that it forms dimers and lower aggregates at concentrations well below the critical micelle concentration. In this respect its behavior compares well with observations of other authors concerning the surfactants with longer than 12 carbon chains[36].

3. Due to the hydrophobically driven aggregation of ORB molecules, the ionized rhodamine B xanthene rings come close to each other and form J- and H-dimers or higher aggregates, which affect the spectroscopic properties. We have found that both J- and H-dimers exist simultaneously in aqueous media together with a non-negligible fraction of higher J-aggre-

gates. In this point, the behavior of ORB differs from that of the parent compound, rhodamine B. The difference can be accounted for by the fact that the ORB head-groups are localized in domains containing hydrophobic CH_2 groups and the polarity of the microenvironment is significantly lower than that of the bulk water, while the rhodamine B molecules are directly solvated by water.

4. The formation of aggregates depends on the probe concentration and may be strongly influenced by ionic strength of the solution. The presence of small ions screens the electrostatic repulsion between positively charged rhodamine B head-groups and promotes aggregation. In addition to the general trends, we observed specific effects with some ions (*e.g.*, ClO_4^-).

5. H-Dimers are not only non-fluorescent, but they act as efficient excitation energy traps and quench strongly the fluorescence of monomer head-groups. The fluorescence intensity is very weak in aqueous media and, as will be demonstrated in the accompanying paper, increases strongly after the binding of ORB to micelles. This fact is very advantageous for FCS applications since the fluorescence from the water-dissolved ORB aggregates, which are in equilibrium with the micelle-bond probes, does not contribute to the monitored fluorescence signal and does not complicate the analysis.

6. In conclusion, the paper shows that ORB is a suitable probe for labeling the polymer nanoparticles and studies of their behavior in aqueous media by FCS.

This study was supported by the Grant Agency of the Czech Republic (grant No. 203/01/0536) and by the Grant Agency of the Charles University (grant No. 215/2000/BCh/Pr). The support of the Ministry of Education, Youth and Sports of the Czech Republic (LN 00A032) is also aknowledged.

REFERENCES

1. Iyi N., Sasai R., Fujita T., Deguchi T., Sota T., Arbeola F. L., Kitamura K.: *Appl. Clay Sci.* **2002**, *22*, 125.
2. Nagao T., Kubo T., Fujimoto R.: *Biochem. J.* **1995**, *307*, 563.
3. Nakashima K., Anzai T., Fujimoto Y.: *Langmuir* **1994**, *10*, 658.
4. Ediger M. D., Dominigue R. P., Fayer M. D.: *J. Chem. Phys.* **1984**, *80*, 1246.
5. Štěpánek M., Humpolíčková J., Procházka K., Hof M., Tuzar Z., Špírková M.: *Collect. Czech. Chem. Commun.* **2003**, *68*, 2120.
6. Magde D., Elson E. L., Webb W. W.: *Phys. Rev. Lett.* **1972**, *29*, 705.
7. Webb W. W. in: *Fluorescence Correlation Spectroscopy. Theory and Applications* (R. Riedler and E. S. Elson, Eds). Springer Verlag, Berlin 2001.
8. Hink M. A., van Hoek A., Visser A. J. W. G.: *Langmuir* **1999**, *15*, 992.
9. Koppel D. E.: *Phys. Rev.* **1974**, *10*, 1938.
10. Kask P., Günter R., Axhausen P.: *Eur. Biophys. J.* **1997**, *25*, 163.

11. Meseth U., Wohland T., Rigler R., Vogel H.: *Biophys. J.* **1999**, *80*, 2987.
12. Edman L.: *J. Phys. Chem. A* **2000**, *104*, 6165.
13. Wohland T., Rigler R., Vogel H.: *Biophys. J.* **2000**, *80*, 2987.
14. Magde D., Elson E. L., Webb W. W.: *Biopolymers* **1974**, *13*, 29.
15. Elson E. L., Magde D.: *Biopolymers* **1974**, *13*, 1.
16. Magde D., Webb W. W., Elson E. L.: *Biopolymers* **1978**, *17*, 361.
17. Aragón S. R., Pecora R.: *Biopolymers* **1975**, *14*, 119.
18. Aragón S. R., Pecora R.: *J. Chem. Phys.* **1976**, *64*, 1791.
19. Hess S. T., Huang S., Heikal A. A., Webb W. W.: *Biochemistry* **2002**, *41*, 697.
20. Thompson N. L. in: *Topics in Fluorescence Spectroscopy* (J. R. Lakowicz, Ed.), Vol. 1, Chap. 6. Plenum Press, New York 1991.
21. Del Monte F., Levy D.: *J. Phys. Chem. B* **1998**, *102*, 8036.
22. Burghardt T. P., Lyke J. E., Ajtai K.: *Biophys. Chem.* **1996**, *59*, 119.
23. Vogel R., Harvey M., Edwards G., Meredith P., Heckenberg N., Trau M., Rubinstein-Dunlop H.: *Macromolecules* **2002**, *35*, 2063.
24. Ray K., Nakahara H.: *J. Phys. Chem. B* **2002**, *106*, 92.
25. Del Monte F., Mackenzie J. D., Levy D.: *Langmuir* **2000**, *16*, 7377.
26. Aguirresacona I. U., Arbeola F. L., Arbeola I. L.: *J. Chem. Educ.* **1989**, *66*, 866.
27. Chaudhuri R., Arbeola F. L., Arbeola I. L.: *Langmuir* **2000**, *16*, 1285.
28. Kemnitz K., Yoshihara K.: *J. Phys. Chem.* **1991**, *95*, 6095.
29. Nakashima K., Fujimoto Y.: *Photochem. Photobiol.* **1994**, *60*, 565.
30. McRae E. G., Kasha M.: *Physical Processes in Radiation Biology*. Academic Press, New York 1964.
31. Kasha M., Rawls H. R., El-Bayoumi A.: *Pure Appl. Chem.* **1965**, *11*, 38.
32. McRae E. G., Kasha M.: *J. Chem. Phys.* **1961**, *11*, 38.
33. Chambers R. W., Kajiwara T., Kearns D. R.: *J. Phys. Chem.* **1974**, *78*, 380.
34. Dunsbach R., Schmidt R.: *J. Photochem. Photobiol., A: Chemistry* **1995**, *85*, 275.
35. Fujii T., Nishikiori H., Tamura T.: *Chem. Phys. Lett.* **1995**, *233*, 424.
36. Mukerjee P.: *J. Phys. Chem.* **1965**, *69*, 2821.
37. MacDonald R. I.: *J. Biol. Chem.* **1990**, *265*, 13533.
38. Štěpánek M., Podhájecká K., Procházka K., Teng Y., Webber S. E.: *Langmuir* **1999**, *15*, 4185.